# Transforming growth factor-β1 functions as a competitive endogenous RNA that ameliorates intracranial hemorrhage injury by sponging microRNA-93-5p

HAN WANG[1,2*], XIANMING CAO[1,3*], XIAOQING WEN[1,3,] DONGLING LI[1,3], YETONG OUYANG[4], BING BAO[1], YUQIN ZHONG[3], ZHENGFANG QIN[3], MIN YIN[3], ZHIYING CHEN[1,5] and XIAOPING YIN[1,5]

[1]Department of Neurology, The Affiliated Hospital of Jiujiang University, Jiujiang, Jiangxi 332000;
[2]Department of Outpatient, The First Affiliated Hospital of Nanchang University; [3]Department of Neurology, The Second Affiliated Hospital of Nanchang University; [4]Department of Neurology, Jiangxi Provincial People's Hospital, Nanchang, Jiangxi 330006; [5]Jiujiang University Clinical Research Center for Precision Medicine and Translational Medicine, Jiujiang, Jiangxi 332000, P.R. China

**Abstract.** Intracerebral hemorrhage (ICH) has the highest mortality rate of all stroke subtypes but an effective treatment has yet to be clinically implemented. Transforming growth factor-β1 (TGF-β1) has been reported to modulate microglia-mediated neuroinflammation after ICH and promote functional recovery; however, the underlying mechanisms remain unclear. Non-coding RNAs such as microRNAs (miRNAs) and competitive endogenous RNAs (ceRNAs) have surfaced as critical regulators in human disease. A known miR-93 target, nuclear factor erythroid 2-related factor 2 (Nrf2), has been shown to be neuroprotective after ICH. It was hypothesized that TGF-β1 functions as a ceRNA that sponges miR-93-5p and thereby ameliorates ICH injury in the brain. Short interfering RNA (siRNA) was used to knock down TGF-β1 and miR-93 expression was also pharmacologically manipulated to elucidate the mechanistic association between miR-93-5p, Nrf2, and TGF-β1 in an *in vitro* model of ICH (thrombin-treated human microglial HMO6 cells). Bioinformatics predictive analyses showed that miR-93-5p could bind to both TGF-β1 and Nrf2. It was found that neuronal miR-93-5p was dramatically decreased in these HMO6 cells, and similar changes were observed in fresh brain tissue from patients with ICH. Most importantly, luciferase reporter assays were used to demonstrate that miR-93-5p directly targeted Nrf2 to inhibit its expression and the addition of the TGF-β1 untranslated region restored the levels of Nrf2. Moreover, an miR-93-5p inhibitor increased the expression of TGF-β1 and Nrf2 and decreased apoptosis. Collectively, these results identified a novel function of TGF-β1 as a ceRNA that sponges miR-93-5p to increase the expression of neuroprotective Nrf2 and decrease cell death after ICH. The present findings provided evidence to support miR-93-5p as a potential therapeutic target for the treatment of ICH.

## Introduction

Intracerebral hemorrhage (ICH) is an important public health problem leading to high rates of death and disability in adults and accounts for 10-15% of all cases of stroke (1). The efficacy of hemostatic therapies for acute, spontaneous ICH is unclear (2) and no effective treatment strategies have been clinically implemented. Recently, investigations have focused on underlying molecular markers correlated with brain injury after ICH onset, which have provided possible therapeutic targets for ICH treatment.

Transforming growth factor-β1 (TGF-β1) is a pleiotropic cytokine that has been shown to regulate a variety of cellular processes such as proliferation, inflammation and apoptosis (3). Among the three isoforms of TGF-β present in mammalian cells (4), TGF-β1 was the first to be discovered and remains the best studied. The dysregulation of the TGF-β pathway leads to

*Correspondence to:* Dr Zhiying Chen or Dr Xiaoping Yin, Department of Neurology, The Affiliated Hospital of Jiujiang University, 57 Xunyang East Road, Jiujiang, Jiangxi 332000, P.R. China
E-mail: chenzhiying@ccmu.edu.cn
E-mail: xiaopingbuxiao@126.com

*Contributed equally

a number of human diseases including cardiovascular disease, tissue fibrosis and cancer (5), demonstrating the essential role of the TGF-β proteins *in vivo*. However, less research has been done on TGF-β in the central nervous system (CNS).

The main sources of TGF-β1 in the injured brain are microglia and astrocytes (6). In 1997, Wyss-Coray *et al* (7) found that the local expression of TGF-β1 within the CNS parenchyma can enhance immune-cell infiltration and intensify the CNS impairment resulting from peripherally triggered autoimmune responses. Conversely, more reports have been published in recent years demonstrating the beneficial effects of TGF on nerve function; it was reported that TGF-β1 could reactivate chronically denervated Schwann cells and could potentially be used to prolong regenerative responses to promote axonal regeneration (8). TGF-β1 expression was increased after acute ischemic brain injury; it decreased infarct volume, increased neurogenesis, and decreased apoptosis in rodent models of ischemic stroke (9,10). Clinical epidemiological data showed that gene polymorphisms of TGF-β1 (G800A and T869C) and their corresponding haploids (that result in decreased TGF-β1 content) significantly increased the risk of ICH in patients (11). The co-treatment of recombinant tissue plasminogen activator with ginsenoside significantly improved outcomes in patients with ICH, which could be attributed to the ginsenoside-induced increase in TGF-β1 (12). Nevertheless, the specific mechanism of TGF-β1 in ameliorating ICH injury has not yet been clearly elucidated.

Nuclear factor erythroid 2-related factor 2 (Nrf2) is a basic-leucine-zipper transcription factor that regulates the expression of antioxidant genes by binding to the antioxidant response element (ARE). Activation of Nrf2 has been shown to ameliorate many systemic fibrosis-associated diseases. One study suggested that Nrf2 inhibited TGF-β1 in hepatic stellate cells (13). More pertinently, Nrf2 was found to be neuroprotective after ICH; several compounds including hemin, dimethyl fumarate and some flavonoids protected against brain injury after ICH via mechanisms involving Nrf2 (14,15). Specifically, microglial Nrf2 increased phagocytosis and hematoma clearance after ICH *in vitro* and *in vivo* (16). Additionally, Nrf2 knockout mice exhibited greater neurological deficits following ICH injury compared with wild-type mice (17). These findings together suggest that Nrf2 expression is closely associated with neuroprotection and improvement following ICH injury.

MicroRNA (miRNA) is a short-sequence non-coding RNA that binds to complementary sequences on target messenger RNA (mRNA) transcripts called miRNA recognition elements (MREs). MREs are often found on the 3' untranslated region (UTR) of the mRNA transcript, and MRE binding by a miRNA usually prevents the mRNA from being translated into protein (18). Following the milestone discovery of miRNAs (19), the subsequent wave of research established a solid association between miRNA dysregulation and human disease. miR-93-5p was found to be associated with inflammation, oxidative stress and cell apoptosis (20,21). Specifically, Nrf2 has been identified as a target of miR-93-5p that, by inhibiting Nrf2 translation, blocks its antioxidant and neuroprotective effects (22,23). miR-93-5p has also been previously associated with the regulation of TGF-β-mediated signaling. One study demonstrated that miR-93-5p inhibited RUNX3,

a member of the TGF-β superfamily, which led to increased invasion and migration of renal carcinoma cells (24). Another study reported that miR-93-5p downregulated a TGF-β1 receptor in nasopharyngeal carcinoma (25) and a third study suggested that miR-93-5p suppressed TGF-β1-induced fibrosis in renal tissue (26). Despite the evidence supporting the influence of miR-93-5p on TGF-β signaling, no one has directly investigated the interaction between miR-93-5p and TGF-β1, certainly not following ICH in the brain.

Competitive endogenous RNAs (ceRNAs) regulate gene expression by competitively binding to miRNAs. For example, the long non-coding RNA (lncRNA) ROR promoted osteogenic differentiation of mesenchymal stem cells by functioning as a ceRNA for miR-138 and miR-145 and could be developed into a therapeutic strategy for bone diseases (27). Similarly, the ceRNA regulatory pathway involving the lncRNA HCAL, miRNAs (miR-15a, -196a, and -196b), and the LAPTM4B gene found in hepatocellular carcinoma (HCC) suggested that ceRNA could be used as a potential therapeutic target for HCC treatment (28). Research on the regulatory mechanisms of ceRNA and their potential for disease treatment is still an actively investigated research topic.

In the present study, it was hypothesized that the 3' untranslated region (UTR) of TGF-β1 functions as a ceRNA that sponges miR-93-5p and thereby ameliorates the effects of ICH injury in the brain. Firstly, it was predicted that the 3'-UTR of TGF-β1 would be able to bind miR-93-5p. Secondly, it was postulated that TGF-β1 expression would be elevated, while miR-93-5p levels would be decreased, in a post-ICH cellular environment. Thirdly, it was predicted that miR-93-5p-mediated inhibition of Nrf2 would be mitigated in the presence of TGF-β1 due to competitive binding. Finally, it was expected that TGF-β1-mediated sponging of miR-93-5p would decrease apoptosis and increase the neuroprotective expression of Nrf2, effectively protecting against ICH-induced brain injury. The present findings revealed a novel TGF-β1/miR-93-5p/Nrf2 ceRNA regulatory pathway and provided new insight into harnessing this molecular mechanism as a potential treatment for ICH.

**Materials and methods**

*Bioinformatic analysis*. TargetScan (http://www.targetscan.org/) and miRTarBase (http://mirtarbase.mbc.nctu.edu.tw/php/index.php) were used to analyze the putative targets of miR-93-5p. The web tool GeneMANIA (29) (http://genemania.org/) was used, which searches an extensive set of functional association data, to determine the association between Nrf2 and TGF-β1 genes.

*Cell culture and treatments*. As previously established, immortalized human microglial cell line HMO6 was used in the present study (30) for the majority of the experiments, purchased from the College of Life Science at Wuhan University (Wuhan, China). The cells were incubated in high-glucose Dulbecco's Modified Eagle's Medium (DMEM/high glucose; GibcoBRL/Invitrogen; Thermo Fisher Scientific, Inc.) supplemented with 10% inactivated fetal bovine serum (FBS; 21103-049; Life Technologies, GibcoBRL/Invitrogen; Thermo Fisher Scientific, Inc.) and 100 U/ml penicillin/streptomycin

Table I. Data collected on patients.

| Case no. | Age, years | Sex | HPI | PH | Sampling site | Type |
|---|---|---|---|---|---|---|
| 1 | 70 | M | Glioma | Hypertension | Left frontal lobe | Cont |
| 2 | 63 | F | Glioma | None | Left thalamus | Cont |
| 3 | 43 | M | Meningioma | Hypertension | Right cerebellopontine angle | Cont |
| 4 | 28 | M | Epilepsy | Fracture | Right frontal lobe | Cont |
| 5 | 64 | M | DLBCL | None | Right parietal lobe | Cont |
| 6 | 49 | F | Epilepsy | None | Left temporal lobe | Cont |
| 7 | 43 | M | Intracerebral hemorrhage | None | Left occipital lobe | ICH |
| 8 | 12 | F | Moyamoya disease | None | Left temporal lobe | ICH |
| 9 | 49 | F | Intracerebral hemorrhage | None | Left occipital lobe | ICH |
| 10 | 47 | M | Moyamoya disease | None | Left frontal lobe | ICH |
| 11 | 54 | F | Cerebral hemorrhage | None | Right cerebellum | ICH |
| 12 | 62 | F | Cerebral hemorrhage | Hypertension | Left cerebellum | ICH |

HPI, history of present illness; PH, patient history; M, male; F, female; DLBCL, diffuse large B-cell lymphoma; Cont, control patient; ICH, intracerebral hemorrhage.

(GibcoBRL/Invitrogen; Thermo Fisher Scientific, Inc.) at 37°C with 5% $CO_2$. When cells were 80% confluent, 0.25% trypsin (Sigma-Aldrich; Merck KGaA) was used for digestion and passaging. To investigate the mechanism of miR-93-5p and TGF-β1 after ICH, cells were treated with thrombin from human plasma (thrombin concentration used as in previous literature; 20 or 40 U/ml; Sigma-Aldrich; Merck KGaA) for 48 h and then harvested for detection (31).

To confirm the regulatory effect of miR-93-5p and the TGF-β1 signaling pathway, HMO6 cells were exposed to thrombin (20 U/ml) for 48 h. Then, cells were transfected for 48 h with either a miR-93 mimic (50 nM), a miR-93 inhibitor (100 nM), a small interfering (si) RNA specific to TGF-β1 (siTGF-β1; 50 nM), or mimic NC, inhibitor NC, and scramble siRNA as the negative control. The mimic, inhibitor, siRNA, and negative-control RNA were sourced from RiboBio Co., Ltd. and used according to the manufacturers' instructions. The transfected cells were measured for levels of miR-93, TGF-β1, and Nrf2.

*Fresh brain tissue.* Fresh brain tissue was taken from 12 adult surgical patients [six females and six males; mean age (range), 48.7 years (12-70 years)] at the Department of Neurosurgery at The Second Affiliated Hospital of Nanchang University. The cohort consisted of equal numbers of patients with and without ICH; Table I describes the details regarding the patients and the collected samples. The tissue was collected in sterile tubes and stored in liquid nitrogen for later experiments. Written informed consent was obtained from all tissue donors or their parent/guardian prior for inclusion in the present study. All the protocols used in the present study were approved by the Ethics Committee at The Second Affiliated Hospital of Nanchang University (Nanchang, China).

*Enzyme-linked immunosorbent assay (ELISA).* The proinflammatory cytokines produced by activated microglia include interleukin (IL)-1β, tumor necrosis factor-α (TNF-α)

and IL-6, which can cause cytotoxic or cytopathogenic effects in the CNS (30). The production of TNF-α in HMO6 cells after a 48-h incubation with thrombin was determined in spent culture supernatants (only the culture media collected) using ELISA kits specific for human TNF-α (cat. no. 5YJ3MQ3F; Elabscience; kit capable of detecting TNF-α at 4.69 pg/ml). At the end of each experiment, culture supernatants were collected, centrifuged and stored at -70°C.

*Double-immunofluorescence staining.* HMO6 cells were fixed for 30 min at room temperature in 4% paraformaldehyde in PBS (pH 7.4), and then permeabilized with 0.25% Triton X-100 for 4 min at room temperature. Slides were incubated for 1 h in 10% goat serum/TBS, followed by incubation with 1:100 dilution of mouse anti-Iba1 antibody (Wako Pure Chemical Industries, Ltd.; cat. no. 012-26723) and 1:50 rabbit anti-CD68 (BIOSS, bs-20403R) at 4°C overnight. Then, the sections were incubated with Alexa 568-conjugated donkey anti-rabbit IgG (red) (1:200 in PTwH; Life Technologies; cat. no. A10042) and Alexa 488-conjugated donkey anti-mouse IgG (green; 1:200 in PTwH; Life Technologies; cat. no. A32766) for 2 h at room temperature. Nuclei were stained with DAPI (Abcam). Microgliosis was assessed by measuring the immunoreactivity of Iba1 (expressed by all microglia) and CD68 (expressed by activated microglia). The images were observed under a fluorescence microscope (Olympus IX71; Olympus Corporation; magnifications, x40 and x20) and Image Pro-Plus 6.0 software (1993, 2003 Media Cybernetics) was applied to calculate the immunohistochemical optical density.

*RNA/miRNA extraction and reverse-transcription quantitative polymerase chain reaction (RT-qPCR).* Total RNA and miRNAs were extracted from fresh brain tissue or cultured HMO6 cells using TRIzol (Takara Bio, Inc.) and the miRNeasy Mini kit (Qiagen GmbH), respectively. miR-93 was reverse-transcribed using a One Step PrimeScript miRNA cDNA synthesis kit (Takara Biotechnology Co., Ltd.)

Table II. Primer sequences for RT-qPCR.

| Gene | Forward, 5'-3 | Reverse, 5'-3' |
| --- | --- | --- |
| miR-93 | CAAAGTGCTGTTCGTGCAGGTAG | GCTGTCAACGATACGCTACG |
| miR-181c | AACATTCAACCTGTCGGTGAGT | GCTGTCAACGATACGCTACG |
| U6 | GATGACACGCAAATTCGTGAA | GCTGTCAACGATACGCTACG |
| TGF-β1 | AGAAGAACTGCTGCGTGCG | TACACGATGGGCAGCGG |
| Nrf2 | CCAGCACATCCAGTCAGAAAC | GTCATCTACAAACGGGAAT |
| TGF-β1 3'UTR | ATCAAGGCACAGGGGACCAG | CTCTGGGCTTGTTTCCTCAC |
| Actin | TGGCACCCAGCACAATGAA | CTAAGTCATAGTCCGCCTAGAAGCA |

miR, microRNA; TGF-β1, transforming growth factor-β1; Nrf2, nuclear factor erythroid-2 related factor 2; RT-qPCR, reverse-transcription-quantitative polymerase chain reaction; UTR, untranslated region.

according to the manufacturer's protocol. qPCR was performed with SYBR Green I Master mix (Roche Diagnostics GmbH) using a LightCycler 480 (Roche Diagnostics) as follows: 94˚C for 2 min, 94˚C for 30 sec, 55˚C for 30 sec, 72˚C for 30 sec, and 72˚C for 2 min. The sequences of the specific primers are listed in Table II. Melting curve analyses confirmed that all the primers were specific for their respective transcripts. Actin and U6 were used as the reference genes. RT-qPCR was adopted to confirm the transfection efficiency. Each reaction was performed at a 10-$\mu$l reaction volume and in triplicate. RT-qPCR data were analyzed using the $2^{-\Delta\Delta Cq}$ method (32), which uses the threshold or quantification cycle (Cq) to generate a relative gene-expression value that is normalized both to the reference gene expression and to the control experimental condition (+/- thrombin).

*Western blotting.* The brain samples or isolated HMO6 cells were mechanically lysed in RIPA lysis buffer (Beyotime Institute of Biotechnology) and an enhanced bicinchoninic protein assay kit was used to measure protein concentrations. The protein samples were then loaded onto a 10% SDS-PAGE gel at 50 $\mu$g per lane and the proteins were separated. Next, the proteins were electrophoretically transferred to a polyvinylidene difluoride membrane (EMD Millipore). The membrane was blocked with 3% BSA (BioSharp Life Sciences) for 1 h at room temperature, followed by an incubation for 12 h at 4˚C with primary antibodies. The primary antibodies used were: Anti-Nrf2 (rabbit polyclonal; 1:1,000 dilution) (cat. no. GTX103322), anti-TGF-β1 (mouse polyclonal; 1:1,000 dilution) (cat. no. GTX45121; both from GeneTex, Inc.) and anti-β-actin (Abcam; cat. no. 8226). After three washes in TBS with 0.1% Tween-20 (TBST), the membrane was probed with horseradish peroxidase (HRP)-conjugated anti-rabbit (1:1,000; Sigma-Aldrich; Merck KGaA; cat. no. A3812) or anti-mouse (1:1,000; Sigma-Aldrich; Merck KGaA; cat. no. A3562) secondary antibodies for 1 h at room temperature. The protein bands were visualized with a SuperSignal West Pico chemiluminescence kit (Thermo Fisher Scientific, Inc.). Finally, ImageJ 1.51j8 software (National Institutes of Health) was used to measure the relative density of the proteins, which was normalized to the loading control β-actin. The experiments were performed in triplicate.

*Dual luciferase reporter assay.* The 3'UTR and coding sequence (CDS) of TGF-β1 were amplified from the genomic DNA of human brain tissue and subcloned into the pcDNA4.0 (Addgene; cat. no. MLCC1153; 5.1kb) or psiCHECK2 (Addgene; cat. no. P0197; 6.3kb) dual luciferase reporter plasmids. Specifically, pcDNA4.0 luciferase reporters containing TGF-β1-CDS (1,173 bp), TGF-β1-3'UTR-WT (729 bp), or TGF-β1-3'UTR-MUT (729 bp; TGF-β1 with a mutated 3'UTR sequence) were constructed. The psiCHECK2 reporters contained either Nrf2 3'UTR (486 bp) or TGF-β1 3'UTR (729 bp). The constructed vectors were transfected into 293T cells and HMO6 cells with Lipofectamine® 3000 Transfection Reagent (Invitrogen; Thermo Fisher Scientific, Inc.). For some experiments, the luciferase reporter plasmids were co-transfected with an miR-93 mimic (or the control; mimic NC), miR-93 inhibitor (or the control; inhibitor NC), siTGF-β1 (5'-AAGGGCTACCATGCCAACTTC-3') (33), or the scramble control siTGF-β1-NC, purchased from RiboBio (Guangzhou RiboBio Co., Ltd.). Luciferase activity was analyzed as previously described (34). Each assay was performed in triplicate.

*Terminal deoxynucleotidyl transferase dUTP nick end labeling (TUNEL) assay.* TUNEL assays were performed with the one step TUNEL kit (Tiangen Biotech Co., Ltd.) according to the manufacturer's instructions. Briefly, the transfected HMO6 cells were fixed at room temperature in 4% paraformaldehyde in PBS on poly-(L-lysine)-coated slides, rinsed with PBS, and permeabilized with 0.1% Triton X-100. Then, the slides were washed with PBS, and the cells were incubated with 50 $\mu$l TUNEL reaction mixture for 1 h at 37˚C in the dark. The TUNEL-stained cells were observed under a confocal laser scanning microscope (Olympus IX71; Olympus Corporation; magnification, x10) using 405-nm excitation and 568-nm emission, and cells with red fluorescence were defined as apoptotic cells.

*Statistical analysis.* All the data are expressed as the means ± SD. Statistical analyses were conducted with GraphPad Prism 6.01 software (GraphPad Software, Inc.). The independent Student's t-test was used to compare differences between two groups. More than three groups were analyzed by one-way analysis of variance followed by multiple comparisons using Tukey's test. Statistical significance for intergroup differences was assessed
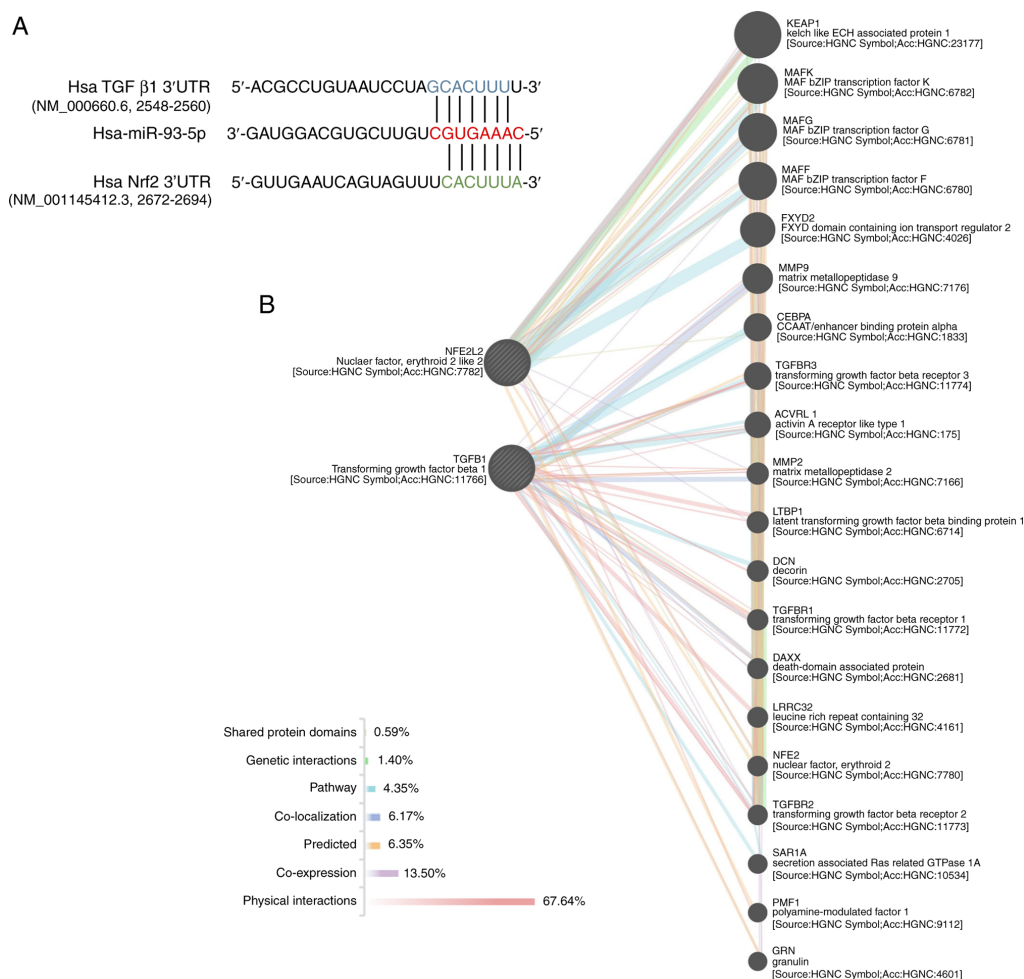
Figure 1. Bioinformatics analysis linking TGF-β1, Nrf2 and miR-93. (A) Association of human (*homo sapiens*; Hsa) TGF-β1 and Nrf2 sharing a common miR-93 binding site on their 3'-UTRs. Two programs (TargetScan and miRTarBase) predicted that both TGF-β1 and Nrf2 were potential targets of the miR-93-5p. The GenBank accession number and base-pair location of the 3'-UTR sequence of TGF-β1 and Nrf2 are included in parentheses. (B) Protein-protein interaction, co-expression network analyses using GeneMANIA. Genes are shown as nodes (gray circles) and color-coded lines indicate seven different types of interactions. The two gray circles on the left depict Nrf2 (also known as NFE2L2) and TGF-β1 (TGFB1) and the gray circles on the right depict the GeneMANIA-predicted genes. A larger gray circle indicates a higher correlation. Numbers represent the percentage of different types of interactions over the total. TGF, transforming growth factor; miR, microRNA; Nrf2, nuclear factor erythroid 2-related factor 2; UTR, untranslated region.

by the $\chi^2$ test or Fisher's exact test for categorical variables. Correlation analysis was performed using the Pearson linear correlation analysis. $P<0.05$ was considered to indicate a statistically significant difference.

## Results

*miR-93-5p targets both TGF-β1 and Nrf2.* A previous study showed that activated Nrf2 could trigger the expression of ARE-regulated heme oxygenase-1 (HO-1), and that Nrf2 played anti-oxidative and anti-inflammatory roles that were neuroprotective following ICH (35). Based on literature reviews and gene-target prediction databases, such as TargetScan and miRTarBase, it was found that miR-93-5p had a binding site on Nrf2 mRNA (context++ score percentile, 85) (22,36). Since TGF-β1 has been heavily investigated as a potential mediator of ICH, its association with miR-93-5p was also analyzed. Bioinformatics analysis using TargetScan and miRTarBase indicated that miR-93-5p bound to the 3'UTR of TGF-β1 mRNA (Fig. 1A). In order to examine the potential connection between TGF-β1, miR-93-5p and Nrf2, GeneMANIA was used

for protein-protein interaction network and gene co-expression analyses. No direct association was found between Nrf2 and TGF-β1 (Fig. 1B), suggesting that miR-93-5p was the association to regulate them both (hereafter miR-93 represents miR-93-5p).

*Relative expression levels of miR-93, TGF-β1 and Nrf2 in HMO6 cells.* Microglia are the resident immune cells of the CNS. After ICH, microglia become activated, obtain an ameboid morphology, and release proinflammatory cytokines (37). A previous study revealed that excessive activation or lack of microglial regulation can cause neurotoxicity (30); microglia are important sources of pro-inflammatory and oxidative-stress factors, such as tumor necrosis factor (TNF), nitric oxide, interleukin and other neurotoxic substances. Therefore, a human microglial cell line (HMO6) was used in the present study as an *in vitro* host and simulated the ICH environment by treatment with thrombin from human plasma. HMO6 cells were treated with thrombin at concentrations of 20 and 40 U/ml and their morphology was visualized under a bright-field
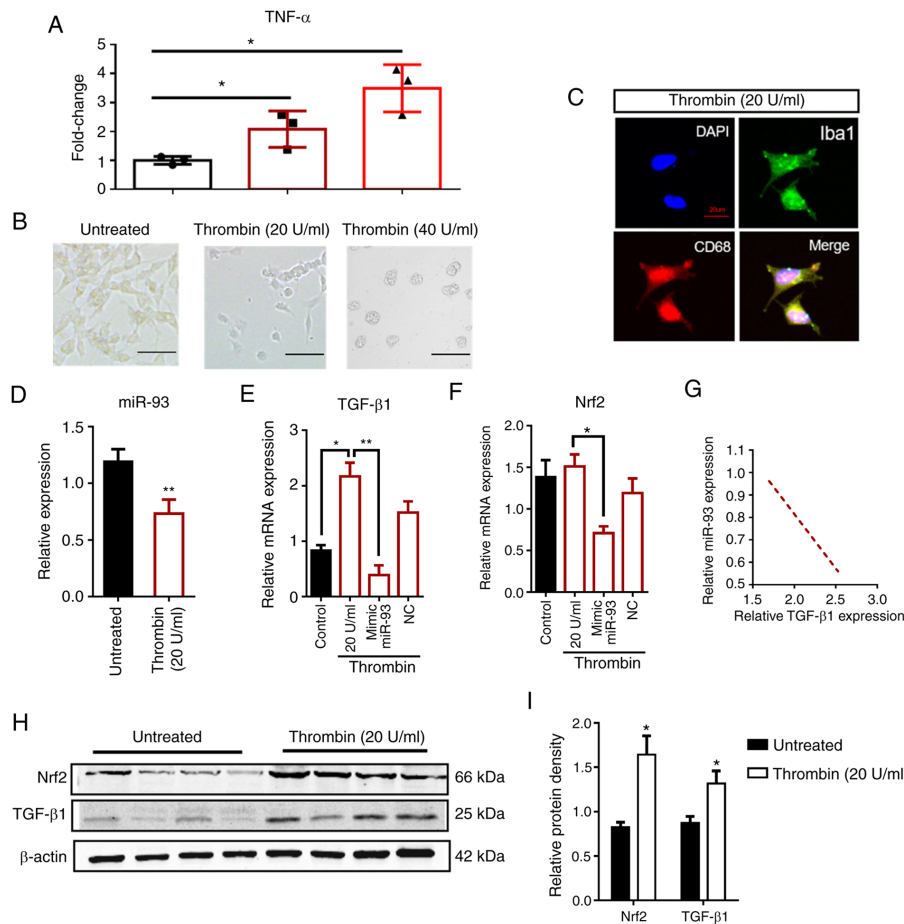
Figure 2. Morphology and expression of HMO6 microglial cells after thrombin treatment. (A) TNF-α mRNA levels in thrombin-treated HMO6 cells are elevated significantly after 48 h, in a dose-dependent manner, compared with control cells (untreated). (B) Phase contrast microscopy showing the morphology of HMO6 cells that are untreated or treated with thrombin at concentrations of 20 or 40 U/ml. Scale bar, 50 $\mu$m. (C) Images of Iba1 (green) and CD68 (red) immunoreactivity in HMO6 cells, treated with 20 U/ml thrombin. DAPI (blue) labels the cell nuclei. Scale bar, 20 $\mu$m. (D) miR-93 expression in HMO6 cells with or without thrombin treatment. (E and F) The modulation of Nrf2 or TGF-β1 mRNA levels in thrombin-treated HMO6 cells after transfection with miR-93 mimic or the corresponding control (mimic NC) was assessed by reverse transcription-quantitative PCR. The red border represents the thrombin-treated groups. (G) TGF-β1 and miR-93 RNA expression levels in HMO6 cells were negatively correlated as assessed by Pearson correlation analysis (r=-0.967; P <0.05). (H) Western blotting images showing the protein levels of TGF-β1 and Nrf2 in HMO6 cells after thrombin (20 U/ml) treatment. β-actin was the loading control. (I) Quantification of the TGF-β1 and Nrf2 protein levels in untreated or thrombin-treated HMO6 cells. n=6 for each group. Data are presented as the means ± SD. *P<0.05, **P<0. 01. TNF, tumor necrosis factor; miR, microRNA; TGF, transforming growth factor; Nrf2, nuclear factor erythroid 2-related factor 2.

microscope (Fig. 2B). In addition, inflammatory factors like TNF-α were detected in the cell supernatants using ELISA kits (Fig. 2A). The expression of TNF-α in cells treated with 40 U/ml thrombin was higher compared with that of cells treated with 20 U/ml thrombin (all P<0.05). This result corresponded with the greater impairment in cellular morphology of the 40 U/ml thrombin-treated cells compared with the 20 U/ml thrombin-treated cells; more cells formed clusters after 40 U/ml thrombin treatment. Despite the higher TNF-α levels implying a more robust ICH-like cellular environment, the highly rounded and clustered microglial cells caused by 40 U/ml thrombin were unsuitable for experiments. Based on the aforementioned findings, HMO6 cells were treat with 20 U/ml thrombin in the subsequent experiments. Furthermore, immunofluorescence staining of Iba1 and CD68 observed in these HMO6 cells revealed that the thrombin treatment successfully activated human microglia (Fig. 2C). By verifying the presence of activated,

ameboid-shaped microglia releasing inflammatory cytokines, an effective *in vitro* model of ICH was established.

Western blotting and RT-qPCR were used to detect changes in miR-93, *TGF-β1*, and *Nrf2* expression in thrombin-treated HMO6 cells. The RT-qPCR results revealed that the expression of miR-93 was decreased (P<0.05), *Nrf2* mRNA levels were not significantly changed, and *TGF-β1* mRNA was significantly elevated (P<0.01) in thrombin-treated cells (Fig. 2D-F). Nrf2 mRNA levels were not significantly changed, whereas Nrf2 protein levels were increased, indicating that the increase in Nrf2 protein levels was regulated by microRNA during translation. After transfection with an miR-93 mimic, the mRNA expression levels of *Nrf2* and *TGF-β1* were both decreased (P<0.05), indicating that miR-93 could negatively regulate both these mRNAs. Pearson's correlation analysis showed that *TGF-β1* (r=-0.967; P<0.05) expression was negatively correlated with miR-93 after ICH (Fig. 2G). The protein levels of Nrf2 and TGF-β1 were increased in thrombin-treated cells (P<0.05; Fig. 2H and I), which further

Table III. Clinical features of patients with ICH and normal controls.

| Baseline characteristics | Controls (n=6) | ICH (n=6) | P-values |
|---|---|---|---|
| Age, mean ± SD years | 52.83±15.82 | 44.50±17.21 | 0.798 |
| Male sex, n% | 66.70 | 33.30 | 0.567 |
| Hypertension, n% | 33.30 | 16.70 | 0.545 |
| Fracture, n% | 16.70 | - | NA |
| Smoking history, n% | 50.00 | 16.70 | 0.545 |

ICH, intracerebral hemorrhage; SD, standard deviation; NA, not available.
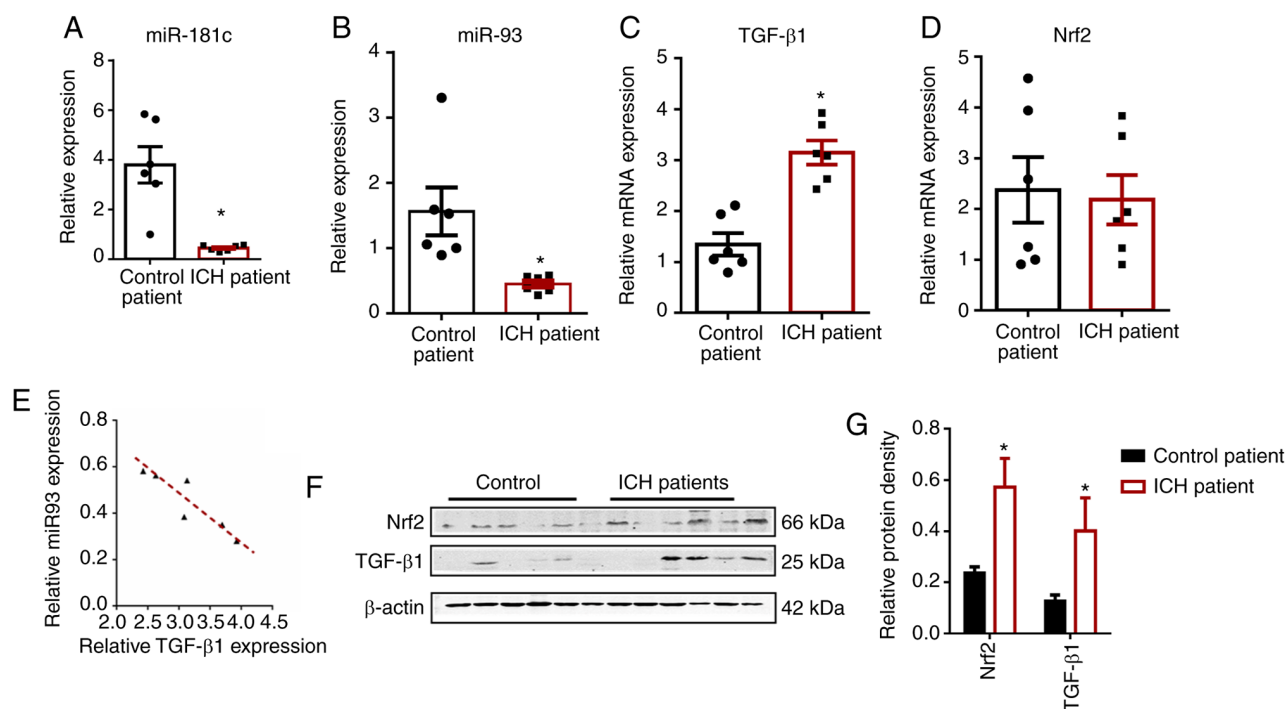


Figure. 3 mRNA and protein expressions of miR93, TGF-s of TGF-β1 and Nrf2 in control and ICH patients. (A) mRNA expression of miRNAs known to be decreased by ICH, miR-181c measured by RT-qPCR in human brain tissue. (B-D) The relative RNA expression of miR-93, TGF-β1 and Nrf2 in patients without ICH (control patients) compared with patients with ICH was detected by RT-qPCR (n=6 for each group). Each individual data point is shown for both groups. The unpaired Student's t-test was used to compare differences. *P<0.05 vs. control patients. (E) TGF-β1 and miR-93 RNA expression levels in human brain tissue were negatively correlated as assessed by Pearson correlation analysis (r=-0.908; P<0.05). (F) A representative western blotting image showing Nrf2 and TGF-β1 protein expressions in human brain tissues. (G) The histogram on the right presents the quantification of the group data. Each experiment was independently repeated at least three times and the data are presented as the means ± SD. *P<0.05. miRNA/miR, microRNA; RT-qPCR, reverse transcription-quantitative PCR; TGF, transforming growth factor; Nrf2, nuclear factor erythroid 2-related factor 2; ICH, intracerebral hemorrhage.

confirmed that both TGF-β1 and Nrf2 were associated with the injury following ICH. The effect of thrombin treatment on Nrf2 protein levels but not mRNA levels suggested that there may be post-transcriptional regulation of Nrf2 after ICH. The significant correlation between miR-93 expression and *TGF-β1* and *Nrf2* expression of thrombin-treated HMO6 cells supports the hypothesis that TGF-β1 functions as a ceRNA by sponging miR-93.

*Expression patterns of miR-93, TGF-β1 and Nrf2 in human brain tissue are consistent with thrombin-treated HMO6 cells.* The demographic characteristics of the participants are shown in Table III. A total of 12 participants with new-onset ICH were recruited into the present study (2 males and 4 females;

median age, 44.50±17.21 years) together with 15 healthy volunteers (4 males and 2 females; median age, 52.83±15.82 years). There was no significant difference in the age or sex distribution between the patients with ICH and healthy volunteers. In order to verify the credibility of the collected human brain tissue, the level of miR-181c was additionally tested, whose decreased expression patterns after ICH have previously been established (Fig. 3A). The results for miR-181c were consistent with previous reports (P<0.05) (38), confirming that the human brain samples were reliable. Detection of mRNA and miRNA expression in the brain tissue of patients with ICH and control (n=6 per group; Table I) revealed that miR-93, *TGF-β1* and *Nrf2* levels were consistent with the expression levels in HMO6 cells. The RT-qPCR results demonstrated
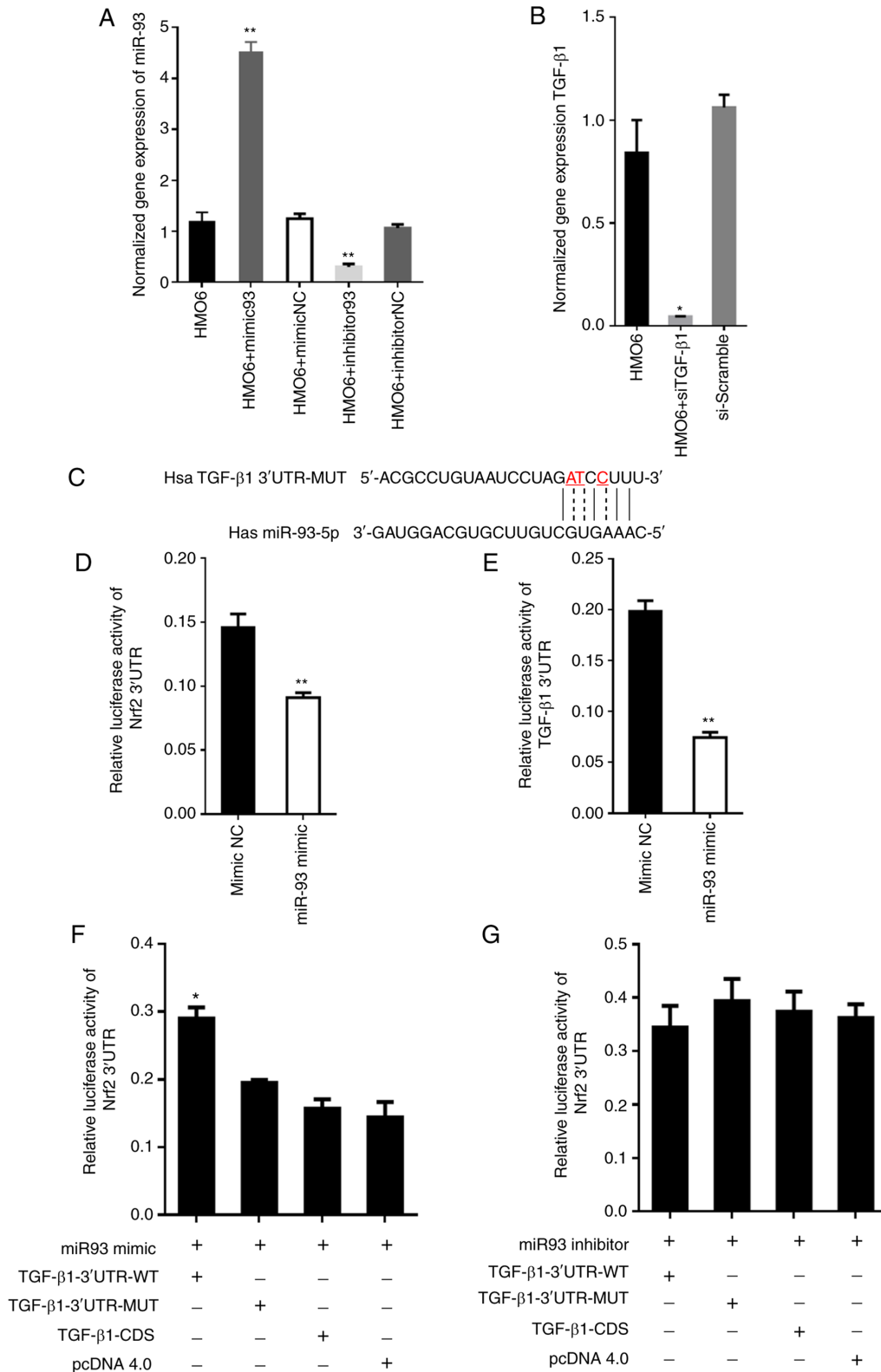
Figure 4. TGF-β1 competes with Nrf2 mRNA for binding to miR-93. (A) Expression of miR-93 in HMO6 cells of each group after transfection. The expression of miR-93 was significantly elevated in miR-93 mimics group and declined in miR-93 inhibitor group, **P<0.05 vs. control group. (B) Expression of *TGF-β1* in HMO6 cells of each group after transfection. The expression of *TGF-β1* was significantly declined in the siTGF-β1 group. *P<0.05 vs. control group. (C) Mutated nucleotides in the *TGF-β1* 3'-UTR sequence (indicated by the dotted line and red font) were generated in the seed region of miR-93 to abolish binding. The mutated sequence is labeled *TGF-β1*-3'-UTR-MUT. (D and E) A dual luciferase reporter assay was used to test whether *TGF-β1* and *Nrf2* were targets of miR-93. 293T cells were co-transfected with (d) *TGF-β1*-3'-UTR or (e) *Nrf2*-3'-UTR and miR-93 mimic or mimic control. **P<0.01. (F) 293T cells were co-transfected with miR-93 mimic + *TGF-β1*-3'UTR-WT, miR-93 mimic + *TGF-β1*-3'-UTR-MUT, miR-93 mimic + *TGF-β1*-CDS, or miR-93 mimic + empty vector pcDNA 4.0. Under these different miR-93/*TGF-β1* conditions, the expression of *Nrf2* was assessed by measuring relative luciferase activity. Data are presented as the means ± SD of three independent experiments. *P<0.05 by Student's t-test. 3'UTR WT is the endogenous 3'-UTR sequence and 3'UTR MUT is the mutated 3'-UTR sequence. (G) The same experimental setup, measures and analyses were conducted as in (F), except with the miR-93 inhibitor. miR, microRNA; RT-qPCR, reverse transcription-quantitative PCR; TGF, transforming growth factor; Nrf2, nuclear factor erythroid 2-related factor 2; si, small interfering RNA; UTR, untranslated region; WT, wild type; MUT, mutant; NC, negative control; CDS, coding DNA sequence.
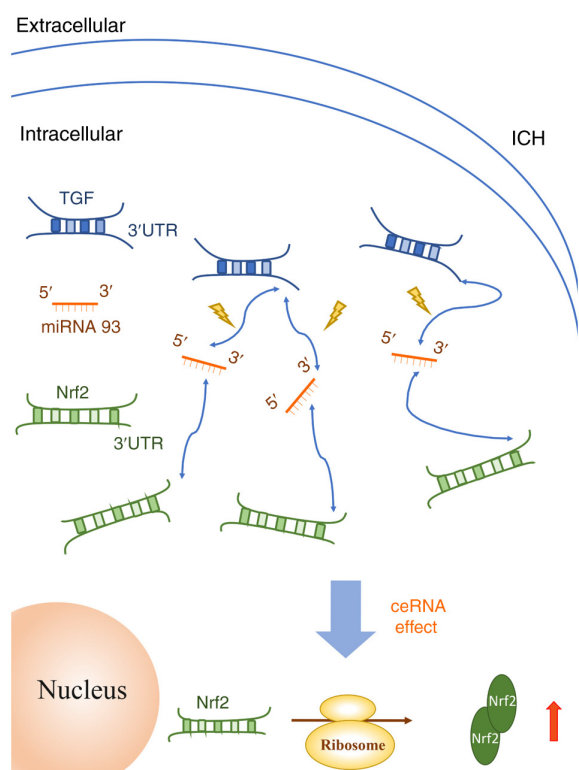
Figure 5. Schematic representation of TGF-β1 function as a ceRNA to regulate Nrf2 after ICH. The TGF-β1 3'-UTR acts as a ceRNA to compete with the Nrf2 3'-UTR for binding to the miR-93. Increased TGF-β1/miR-93 binding leaves Nrf2 mRNA free to be translated. Increased expression of the Nrf2 protein is neuroprotective after ICH. ceRNA, competitive endogenous RNA; ICH, intracerebral hemorrhage; TGF, transforming growth factor; Nrf2, nuclear factor erythroid 2-related factor 2; UTR, untranslated region; miRNA/miR, microRNA.

that the expression of miR-93 was markedly lower, *Nrf2* did not change, and *TGF-β1* expression was significantly higher (P<0.05) in ICH brain tissue compared with the corresponding non-ICH control tissue (Fig. 3B-D); this pattern was consistent with the trend of expression in the thrombin-exposed HMO6 cells. In addition, Pearson's correlation analysis revealed a negative correlation between *TGF-β1* expression and miR-93 after ICH (r, -0.908; P<0.05; Fig. 3E).

Western blotting (Fig. 3F and G) data showed that the protein expression of TGF-β1 and Nrf2 in the tissue from patients with ICH was significantly higher compared with that in control tissue (P<0.05); this post-translational expression pattern was also consistent with that of the ICH model in HMO6 cells.

*TGF-β1 3'UTR functions as a ceRNA by sponging miR-93.* After transfection, the relative expression level of miR-93 was measured via RT-qPCR, to verify transfection efficiency. The results demonstrated that the expression of miR-93 in HMO6 cells of the miR-93 mimics group was markedly elevated when compared with the control groups (P<0.05), and declined in miR-93 inhibitor group (P<0.05). However, the expression of *TGF-β1* decreased significantly in the siTGF-β1 group in comparison with the control groups (P<0.05; Fig. 4A and B). Considering that TGF-β1 and Nrf2 mRNA were predicted targets of miR-93, and that miR-93

showed low expression in brain tissue from patients with ICH, it was hypothesized that TGF-β1 mRNA may act as a ceRNA for miR-93. In order to examine the potential ceRNA function of TGF-β1, a dual luciferase reporter assay was used to directly test whether Nrf2 and TGF-β1 are targets of miR-93. The results showed that luciferase activity was decreased in 293T cells co-transfected with miR-93 and Nrf2-3'UTR or TGF-β1-3'UTR (P<0.01; Fig. 4C-E), indicating that miR-93 could negatively regulate both; this result corroborated what was predicted by the bioinformatics analysis: miR-93 targets both Nrf2 and TGF-β1 mRNA. To determine whether miR-93 acts as a bridge between TGF-β1 and Nrf2 and to support the hypothesized ceRNA function of TGF-β1, a miR-93 mimic or inhibitor was used to simulate in 293T cells an environment with or without miR-93 and measured luciferase activity. As shown in Fig. 4F, the luciferase activity of Nrf2-3'UTR increased when co-transfected with TGF-β1-3'UTR-WT, which offset the negative regulation of miR-93 mimic on Nrf2 (Fig. 4D). However, in the TGF-β1-3'UTR-MUT and in the context of inhibitor 93, this effect disappeared (Fig. 4F and G). Co-transfection of the miR-93 mimic and the coding sequence of TGF-β1 (TGF-β1-CDS) in 293T cells also failed to increase the luciferase activity of Nrf2-3'UTR (Fig. 4F), indicating that the coding region of TGF-β1 has no direct effect on the expression of Nrf2. These results indicate that the comprehensive mechanism by which TGF-β1 3'UTR increased Nrf2 expression was the sponging or competitive binding of miR-93; TGF-β1 competitively binds to miR-93-5p with *Nrf2*. When *TGF-β1* competitively binds to miR-93-5p, the activity of miR-93 decreases, thereby upregulating the expression of Nrf2 (Fig. 5).

*Effects of miR-93 and TGF-β1 on the apoptosis of HMO6 cells.* Next, the functional role of miR-93 after ICH was investigated by artificially overexpressing miR-93 (via miR-93 mimic) or knocking it down (with the miR-93 inhibitor) in thrombin-treated HMO6 cells. The results of western blot analysis showed that both Nrf2 and TGF-β1 protein levels were decreased in cells transfected with the miR-93 mimic (P<0.05; Fig. 6A), which is consistent with the luciferase assay results (Fig. 4D and E). Nrf2 and TGF-β1, which are neuroprotective against ICH, were elevated in cells transfected with an inhibitor of miR-93 (P<0.05). This result suggested that miR-93 inhibited Nrf2 and TGF-β1 and can thereby aggravate brain damage after ICH (Fig. 6B). The loss of TGF-β1 was also simulated using siRNA technology and found that Nrf2 expression was decreased in siTGF-β1-transfected cells compared with those transfected with the scramble control (P<0.05; Fig. 6C). The experiment confirmed that Nrf2 expression is inhibited by miR-93 when TGF-β1 is unavailable to competitively bind or sponge miR-93.

TUNEL staining showed that thrombin control compared with siTGF-β1 and miR-93 mimic-transfected HMO6 cells exhibited enhanced apoptosis (P<0.05). However, the number of TUNEL-positive cells in the miR-93 inhibitor-transfected group was significantly lower than the thrombin group (20 U/ml) and even further decreased compared with the miR-93 mimic and siTGF-β1-transfected groups (P<0.05; Fig. 6D). Collectively, the findings revealed that miR-93
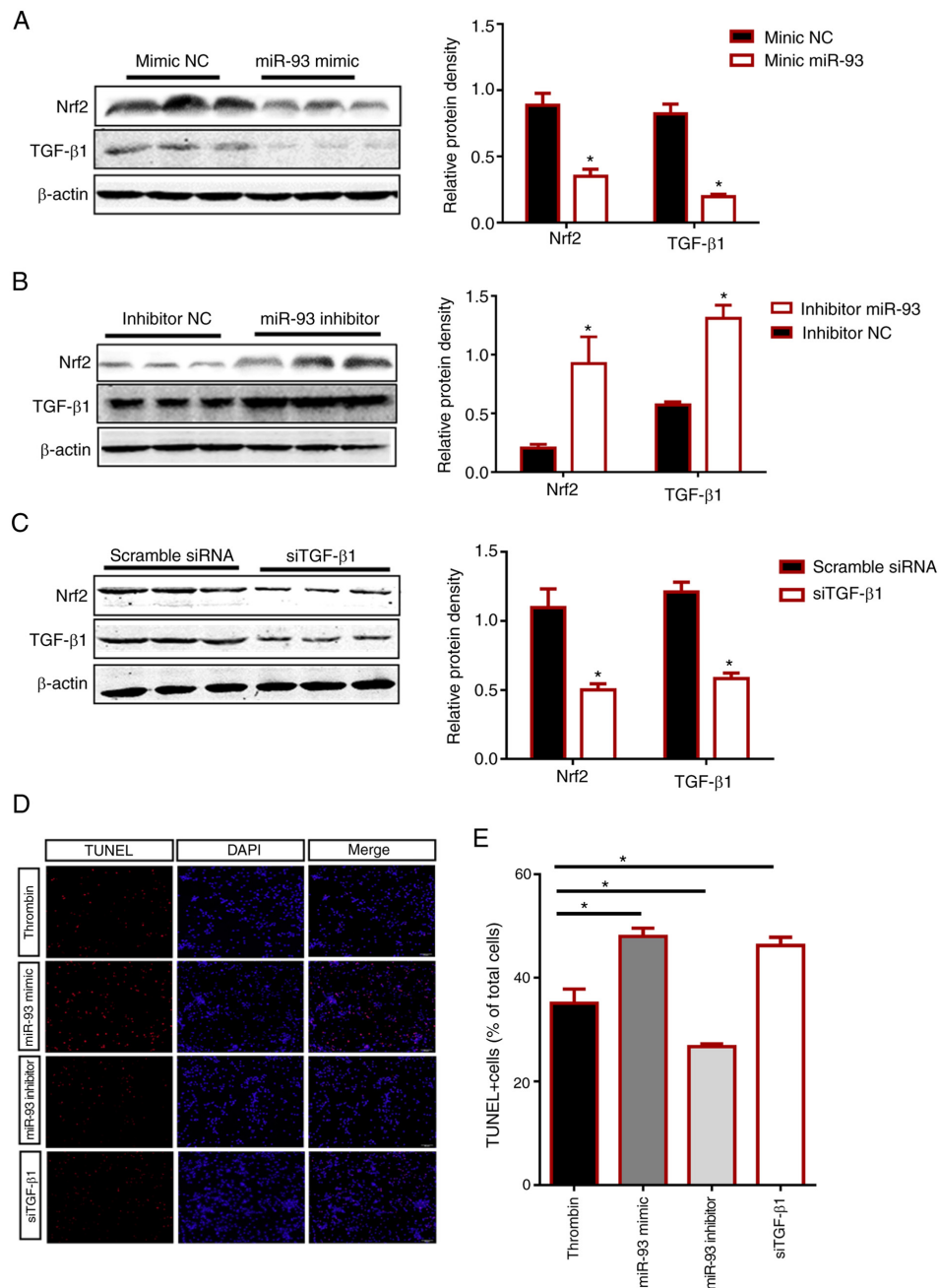
Figure 6. Effects of manipulating miR-93 and TGF-β1 levels on Nrf2 expression and apoptosis. (A-C) Protein expression levels of TGF-β1 and Nrf2 in HMO6 cells transfected for 48 h with (A) miR-93 mimic, (B) miR-93 inhibitor or (C) siTGF-β1 were determined by western blotting. The negative controls in (A), (B), and (C) are mimic NC, inhibitor NC and scramble siRNA, respectively. Representative western blotting images and quantification of the group data are shown. (D) HMO6 cells were treated with 48 h of thrombin treatment (20 U/ml). Then, apoptotic cell death was measured by counting TUNEL-stained cells (red) after transfection with miR-93 mimic, miR-93 inhibitor or siTGF-β1. DAPI (blue) labels cell nuclei. Scale bar, 100 $\mu$m. (E) The bar graph quantifies the number of TUNEL-positive (TUNEL+) cells in the different groups as a percentage of total cells. The group data represent three separate experiments and are expressed as the means ± SD. *$P<0.05$ by Student's t-test. miR, microRNA; TGF, transforming growth factor; Nrf2, nuclear factor erythroid 2-related factor 2; si, small interfering RNA; NC, negative control.

inhibited TGF-β1 and Nrf2 expression and aggravated cellular apoptosis after ICH.

## Discussion

The ceRNA mechanism was first proposed by PierPaolo Pandolfi (39) of Harvard Medical School in a study published in Cell in 2011. This newly discovered gene-expression regulator competed with target mRNA for competitive binding to the same miRNA molecule, resulting in a relative decrease in

the activity of the miRNA. The decreased miRNA activity upregulated the expression level of the miRNA's target genes and played a regulatory role in post-transcriptional gene expression. Since the discovery of ceRNAs, these regulatory molecules have been proposed as therapeutic targets for human diseases. Most research on ceRNA regulatory mechanisms has focused on tumors and A previous study showed that ceRNA may provide novel therapeutic options for ischemic stroke (40)

Various types of RNA molecules, such as pseudo-gene transcripts, long-chain non-coding RNA (lncRNA) and

mRNA, can act as ceRNA to shield the inhibition or degradation of another mRNA by miRNA (39). Those mRNAs that contain complementary binding regions to the miRNA seed sequence [often at the 3'-UTR since it retains the miRNA binding site (18)] are highly likely to be involved in gene regulation by acting as ceRNAs. Considering that the amount of mRNA in the cell exceeds most other types of cellular RNA, and the target sequences of miRNA are mostly located on mRNA, it is reasonable to propose that mRNAs are critical competitors for miRNA binding. In addition, it was found that 3'UTRs on mRNAs not only act as cis regulatory elements that alter the stability of their own mRNA transcripts but may also act in trans to modulate gene expression through miRNA binding (41,42). This is particularly relevant given the recent identification of 3'-UTRs that are expressed independently from the protein-coding sequences to which they are normally linked (43). Nevertheless, most studies investigated lncRNA that function as ceRNA and few studies have focused on 3'UTRs as ceRNA (44,45)

Based on the expression patterns of TGF-β1, Nrf2 and miR-93 that were observed in the brain tissue of patients with ICH, it was hypothesized that the 3'-UTR of TGF-β1 acted as a ceRNA sponge for miR-93, impairing its inhibitory effect on Nrf2 and promoting Nrf2 expression. miR-93 was markedly downregulated under ICH conditions in human brain tissue and in a human microglial cell line. The consequent increase in Nrf2 expression ameliorated ICH injury, as indicated by the decrease in apoptosis that was observed in the *in vitro* model of ICH. Importantly, it was revealed that two neuroprotective factors, TGF-β1 and Nrf2, are associated with miR-93 and are mutually regulated following ICH via a ceRNA-mediated mechanism.

As a multifunctional cytokine, TGF-β1 is expressed by neurons, astrocytes and microglia in the CNS, where it regulates astrocytic regeneration and differentiation and neuronal survival. Clinical studies found that the plasma TGF-β1 level was closely associated with the prognosis of patients with ICH, suggesting that TGF-β1 could promote the recovery of neurological function. The literature indicates that TGF-β1 is closely associated with ICH-induced inflammatory injury, but it remains unclear whether TGF-β1 could directly protect neurons (46). The present study presents the first report of a ceRNA regulatory mechanism in ICH, based on the competitive sponging activity of TGF-β1.

Regarding the association between TGF-β1 and miR-93, there have been reports that miR-93 promoted the TGF-β-induced epithelial-to-mesenchymal transition via the downregulation of NEDD4L in lung cancer cells (47). However, there were no prior studies indicating the correlation between miR-93 and TGF-β1 expression in the brain. In the present study, a mechanism of action for miR-93 in ICH was established and a more comprehensive understanding of how miR-93 aggravated brain damage during ICH was established. Specifically, miR-93 was shown to directly bind the 3'UTR of Nrf2 (predicted by bioinformatics and confirmed by luciferase assay). The downregulation of miR-93 increased the expression of Nrf2, consistent with previous reports (22).

Previous research confirmed that HO-1 inhibited the nuclear translocation of the NF-κB p65 subunit to block the cascade of many downstream inflammatory factors, thereby increasing the nuclear translocation of Nrf2 and resulting in a neuroprotective effect on early brain damage caused by ICH (48). Other studies indicated that Nrf2 in microglia augmented antioxidative capacity, phagocytosis and hematoma clearance after ICH (16). In corroboration, the present data showed that increasing Nrf2 expression by inhibition of miR-93 decreased apoptosis in human microglial cells.

The present study has some limitations. Firstly, only the existence of the TGF-β1/miR-93/Nrf2 pathway in humans was confirmed. The present study did not harness the power of animal models to examine the effects of miR-93 on neurological behaviors, hematoma size, or prognosis after ICH. However, it is not often that a promising point of therapeutic intervention is verified in humans; our results are not restricted by the ever-present question of translation/replication from animals to humans. Future attempts to manipulate the ceRNA function of TGF-β1 as a potential ICH treatment would be strengthened by the knowledge that the mechanism exists in humans and can therefore be clinically applied. Secondly, some studies have used a treated HMO6 cell line to reflect the human brain injury (49,50); but there are still others, such as SH-SY5Y cell line or primary neurons, that can perform similar experiments. The reason why HMO6 cells were used is that most of the evidence suggests that microglia cells are activated shortly after ICH and this activation contributes to secondary ICH-induced brain injury. The HMO6 cell line as human microglia are closer to the present study's experimental principle. The *in vitro* thrombin-toxicity model of ICH in primary human microglia cultured from resected brain tissue may not fully reflect the post-ICH changes in human microglia or other brain cell types *in vivo*. Furthermore, since the patient samples are limited, the present study failed to assess apoptosis in the patient samples. Finally, it is important to note that the control samples of human brain tissue did not represent a healthy brain environment. The patients who provided the control brain tissue did not have ICH but did exhibit other serious diseases, including epilepsy and glioma. Therefore, it is possible that these neurological diseases influenced the expression levels of Nrf2, TGF-β1 and miR-93, making the measurements an inaccurate baseline for comparison with the ICH condition. Nevertheless, the relatively even distribution of diseases and sampling locations strengthened the justification for a "non-ICH" control group.

In summary, the present study elucidated a novel function of TGF-β1, miR-93 and Nrf2 in ICH. The ceRNA mechanism activated following ICH involved the 3'UTR of TGF-β1 serving as a ceRNA to sponge miR-93, thereby increasing the expression of Nrf2 and decreasing apoptosis. The TGF-β1/miR-93/Nrf2 pathway could provide novel opportunities for ICH treatment; for instance, neuroprotection could be achieved by artificially increasing TGF-β1 expression in a localized manner or decreasing miR-93 expression after ICH to increase the expression of Nrf2. The next step towards a potential drug target is the verification of the TGF-β1, Nrf2 and miR-93 binding sites. Future challenges will be to understand why such ceRNA regulatory networks exist, how they may have evolved (perhaps via pseudogenes), and the consequences of perturbing them.

## Acknowledgements

## Availability of data and materials

The datasets used and/or analyzed during the current study are available from the corresponding author on reasonable request.

## Authors' contributions

HW, XC, XW and ZC performed the experiments. DL, YO, BB, YZ, ZQ and MY analyzed the data. ZC and XY designed the study. HW and ZC confirm the authenticity of all the raw data. All authors read and approved the final manuscript.

## Ethics approval and consent to participate

The present study was performed in accordance with the recommendations outlined in the Guide for the Care and Use of Laboratory Animals and in accordance with the National Institutes of Health, and was approved by the Committee on the Ethics of Affiliated Hospital of Jiujiang University (permit no. 2017001). Written informed consent was obtained from all tissue donors or their parent/guardian prior for inclusion in the present study.

## Patient consent for publication

Not applicable.

## Competing interests

The authors declare that they have no competing interests.

## References

1. Qureshi AI, Tuhrim S, Broderick JP, Batjer HH, Hondo H and Hanley DF: Spontaneous intracerebral hemorrhage. N Engl J Med 344: 1450-1460, 2001.
2. Al-Shahi Salman R, Law ZK, Bath PM, Steiner T and Sprigg N: Haemostatic therapies for acute spontaneous intracerebral haemorrhage. Cochrane Database Syst Rev 4: CD005951, 2018.
3. Moses HL, Roberts AB and Derynck R: The discovery and early days of TGF-β: A historical perspective. Cold Spring Harb Perspect Biol 8: a021865, 2016.
4. Esebanmen GE and Langridge WHR: The role of TGF-beta signaling in dendritic cell tolerance. Immunol Res 65: 987-994, 2017.
5. Gordon KJ and Blobe GC: Role of transforming growth factor-beta superfamily signaling pathways in human disease. Biochim Biophys Acta 1782: 197-228, 2008.
6. Brionne TC, Tesseur I, Masliah E and Wyss-Coray T: Loss of TGF-beta 1 leads to increased neuronal cell death and microgliosis in mouse brain. Neuron 40: 1133-1145, 2003.
7. Wyss-Coray T, Borrow P, Brooker MJ and Mucke L: Astroglial overproduction of TGF-beta 1 enhances inflammatory central nervous system disease in transgenic mice. J Neuroimmunol 77: 45-50, 1997.
8. Sulaiman W and Nguyen DH: Transforming growth factor beta 1, a cytokine with regenerative functions. Neural Regen Res 11: 1549-1552, 2016.
9. Ma M, Ma Y, Yi X, Guo R, Zhu W, Fan X, Xu G, Frey WH II and Liu X: Intranasal delivery of transforming growth factor-beta1 in mice after stroke reduces infarct volume and increases neurogenesis in the subventricular zone. BMC Neurosci 9: 117, 2008.
10. Buisson A, Lesne S, Docagne F, Ali C, Nicole O, MacKenzie ET and Vivien D: Transforming growth factor-beta and ischemic brain injury. Cell Mol Neurobiol 23: 539-550, 2003.
11. Kumar P, Kumar A, Misra S, Sagar R, Farooq M, Kumari R, Vivekanandhan S, Srivastava AK and Prasad K: Association of transforming growth factor-β1 gene C509T, G800A and T869C polymorphisms with intracerebral hemorrhage in North Indian Population: A case-control study. Neurol Sci 37: 353-359, 2016.
12. Chen J, Bai Q, Zhao Z, Sui H and Xie X: Ginsenoside represses symptomatic intracerebral hemorrhage after recombinant tissue plasminogen activator therapy by promoting transforming growth factor-beta1. J Stroke Cerebrovasc Dis 25: 549-555, 2016.
13. Zeng J, Chen Y, Ding R, Feng L, Fu Z, Yang S, Deng X, Xie Z and Zheng S: Isoliquiritigenin alleviates early brain injury after experimental intracerebral hemorrhage via suppressing ROS- and/or NF-κB-mediated NLRP3 inflammasome activation by promoting Nrf2 antioxidant pathway. J Neuroinflammation 14: 119, 2017.
14. Zhao X, Sun G, Zhang J, Ting SM, Gonzales N and Aronowski J: Dimethyl fumarate protects brain from damage produced by intracerebral hemorrhage by mechanism involving nrf2. Stroke 46: 1923-1928, 2015.
15. Chang CF, Cho S and Wang J: (-)-Epicatechin protects hemorrhagic brain via synergistic Nrf2 pathways. Ann Clin Transl Neurol 1: 258-271, 2014.
16. Zhao X, Sun G, Ting SM, Song S, Zhang J, Edwards NJ and Aronowski J: Cleaning up after ICH: The role of Nrf2 in modulating microglia function and hematoma clearance. J Neurochem 133: 144-152, 2015.
17. Zhao X, Sun G, Zhang J, Strong R, Dash PK, Kan YW, Grotta JC and Aronowski J: Transcription factor Nrf2 protects the brain from damage produced by intracerebral hemorrhage. Stroke 38: 3280-3286, 2007.
18. Bartel DP: MicroRNAs: Target recognition and regulatory functions. Cell 136: 215-233, 2009.
19. Lee RC, Feinbaum RL and Ambros V: The C. elegans heterochronic gene lin-4 encodes small RNAs with antisense complementarity to lin-14. Cell 75: 843-854, 1993.
20. Singh B, Ronghe AM, Chatterjee A, Bhat NK and Bhat HK: MicroRNA-93 regulates NRF2 expression and is associated with breast carcinogenesis. Carcinogenesis 34: 1165-1172, 2013.
21. Fabbri E, Borgatti M, Montagner G, Bianchi N, Finotti A, Lampronti I, Bezzerri V, Dechecchi MC, Cabrini G and Gambari R: Expression of microRNA-93 and Interleukin-8 during Pseudomonas aeruginosa-mediated induction of proinflammatory responses. Am J Respir Cell Mol Biol 50: 1144-1155, 2014.
22. Wang P, Liang X, Lu Y, Zhao X and Liang J: MicroRNA-93 downregulation ameliorates cerebral ischemic injury through the Nrf2/HO-1 defense pathway. Neurochem Res 41: 2627-2635, 2016.
23. Larki P, Ahadi A, Zare A, Tarighi S, Zaheri M, Souri M, Zali MR, Ghaedi H and Omrani MD; Up-regulation of miR-21, miR-25, miR-93, and miR-106b in gastric cancer. Iran Biomed J 22: 367-373, 2018.
24. Parodi AS, De Guerrero LB, Astarloa L, Cintora A, Gonzalez CC, Maglio F, Magnoni C, Milani H, Ruggiero H and Squassi G: Immunization against Argentinian hemorrhagic fever using an attenuated strain of Junin virus. IV. Evaluation of clinical and immunological results. Medicina (B Aires) 30: 1-3, 1970 (In Spanish).
25. Lyu X, Fang W, Cai L, Zheng H, Ye Y, Zhang L, Li J, Peng H, Cho WC, Wang E, *et al*: TGFβR2 is a major target of miR-93 in nasopharyngeal carcinoma aggressiveness. Mol Cancer 13: 51, 2014.
26. Ma J, Zhang L, Hao J, Li N, Tang J and Hao L: Up-regulation of microRNA-93 inhibits TGF-β1-induced EMT and renal fibrogenesis by down-regulation of Orai1. J Pharmacol Sci 136: 218-227, 2018.

27. Feng L, Shi L, Lu YF, Wang B, Tang T, Fu WM, He W, Li G and Zhang JF: Linc-ROR promotes osteogenic differentiation of mesenchymal stem cells by functioning as a competing endogenous RNA for miR-138 and miR-145. Mol Ther Nucleic Acids 11: 345-353, 2018.
28. Xie CR, Wang F, Zhang S, Wang FQ, Zheng S, Li Z, Lv J, Qi HQ, Fang QL, Wang XM, et al: Long noncoding RNA HCAL facilitates the growth and metastasis of hepatocellular carcinoma by acting as a ceRNA of LAPTM4B. Mol Ther Nucleic Acids 9: 440-451, 2017.
29. Montojo J, Zuberi K, Rodriguez H, Bader GD and Morris Q: GeneMANIA: Fast gene network construction and function prediction for Cytoscape. F1000 Res 3: 153, 2014.
30. Nagai A, Nakagawa E, Hatori K, Choi HB, McLarnon JG, Lee MA and Kim SU: Generation and characterization of immortalized human microglial cell lines: Expression of cytokines and chemokines. Neurobiol Dis 8: 1057-1068, 2001.
31. Wang MD, Wang Y, Xia YP, Dai JW, Gao L, Wang SQ, Wang HJ, Mao L, Li M, Yu SM, et al: High serum MiR-130a levels are associated with severe perihematomal edema and predict adverse outcome in acute ICH. Mol Neurobiol 53: 1310-1321, 2016.
32. Livak KJ and Schmittgen TD: Analysis of relative gene expression data using real-time quantitative PCR and the 2(-Delta Delta C(T)) Method. Methods 25: 402-408, 2001.
33. Qi W, Chen X, Holian J, Mreich E, Twigg S, Gilbert RE and Pollock CA: Transforming growth factor-beta1 differentially mediates fibronectin and inflammatory cytokine expression in kidney tubular cells. Am J Physiol Renal Physiol 291: F1070-F1077, 2006.
34. Wang X, Liu D, Huang HZ, Wang ZH, Hou TY, Yang X, Pang P, Wei N, Zhou YF, Dupras MJ, et al: A novel microRNA-124/PTPN1 signal pathway mediates synaptic and memory deficits in alzheimer's disease. Biol Psychiatry 83: 395-405, 2018.
35. Yin XP, Wu D, Zhou J, Chen ZY, Bao B and Xie L: Heme oxygenase 1 plays role of neuron-protection by regulating Nrf2-ARE signaling post intracerebral hemorrhage. Int J Clin Exp Pathol 8: 10156-10163, 2015.
36. Liu Z, Zhang F, Zhao L, Zhang X, Li Y and Liu L: Protective effect of pravastatin on myocardial ischemia reperfusion injury by regulation of the miR-93/Nrf2/ARE signal pathway. Drug Des Devel Ther 14: 3853-3864, 2020.
37. Taylor RA and Sansing LH: Microglial responses after ischemic stroke and intracerebral hemorrhage. Clin Dev Immunol 2013: 746068, 2013.
38. Yin M, Chen Z, Ouyang Y, Zhang H, Wan Z, Wang H, Wu W and Yin X: Thrombin-induced, TNFR-dependent miR-181c downregulation promotes MLL1 and NF-κB target gene expression in human microglia. J Neuroinflammation 14: 132, 2017.
39. Salmena L, Poliseno L, Tay Y, Kats L and Pandolfi PP: A ceRNA hypothesis: The Rosetta Stone of a hidden RNA language? Cell 146: 353-358, 2011.
40. Chen F, Zhang L, Wang E, Zhang C and Li X: LncRNA GAS5 regulates ischemic stroke as a competing endogenous RNA for miR-137 to regulate the Notch1 signaling pathway. Biochem Biophys Res Commun 496: 184-190, 2018.
41. Rastinejad F and Blau HM: Genetic complementation reveals a novel regulatory role for 3' untranslated regions in growth and differentiation. Cell 72: 903-917, 1993.
42. Rastinejad F, Conboy MJ, Rando TA and Blau HM: Tumor suppression by RNA from the 3' untranslated region of alpha-tropomyosin. Cell 75: 1107-1117, 1993.
43. Mercer TR, Wilhelm D, Dinger ME, Soldà G, Korbie DJ, Glazov EA, Truong V, Schwenke M, Simons C, Matthaei KI, et al: Expression of distinct RNAs from 3' untranslated regions. Nucleic Acids Res 39: 2393-2403, 2011.
44. Fang L, Du WW, Yang X, Chen K, Ghanekar A, Levy G, Yang W, Yee AJ, Lu WY, Xuan JW, et al: Versican 3'-untranslated region (3'-UTR) functions as a ceRNA in inducing the development of hepatocellular carcinoma by regulating miRNA activity. FASEB J 27: 907-919, 2013.
45. Fan Z, Kim S, Bai Y, Diergaarde B and Park HJ: 3'-UTR shortening contributes to Subtype-Specific cancer growth by breaking stable ceRNA crosstalk of housekeeping genes. Front Bioeng Biotechnol 8: 334, 2020.
46. Taylor RA, Chang CF, Goods BA, Hammond MD, Mac Grory B, Ai Y, Steinschneider AF, Renfroe SC, Askenase MH, McCullough LD, et al: TGF-β1 modulates microglial phenotype and promotes recovery after intracerebral hemorrhage. J Clin Invest 127: 280-292, 2017.
47. Qu MH, Han C, Srivastava AK, Cui T, Zou N, Gao ZQ and Wang QE: miR-93 promotes TGF-β-induced epithelial-to-mesenchymal transition through downregulation of NEDD4L in lung cancer cells. Tumour Biol 37: 5645-5651, 2016.
48. Yin XP, Chen ZY, Zhou J, Wu D and Bao B: Mechanisms underlying the perifocal neuroprotective effect of the Nrf2-ARE signaling pathway after intracranial hemorrhage. Drug Des Devel Ther 9: 5973-5986, 2015.
49. Sheikh AM, Yano S, Mitaki S, Haque MA, Yamaguchi S and Nagai A: A Mesenchymal stem cell line (B10) increases angiogenesis in a rat MCAO model. Exp Neurol 311: 182-193, 2019.
50. Narantuya D, Nagai A, Sheikh AM, Masuda J, Kobayashi S, Yamaguchi S and Kim SU: Human microglia transplanted in rat focal ischemia brain induce neuroprotection and behavioral improvement. PLoS One 5: e11746, 2010.